SUPPLEMENTARY INFORMATION

Combined Analysis of Metabolome, Proteomes, and Transcriptomes of HCV-infected Cells and Liver to Identify Pathways Associated With Disease Development

Joachim Lupberger[1,2], Tom Croonenborghs[3,4,5], Armando Andres Roca Suarez[1,2], Nicolaas Van Renne[1,2], Frank Jühling[1,2], Marine A. Oudot[1,2], Alessia Virzì[1,2], Simonetta Bandiera[1,2], Carole Jamey[2,6], Gergö Meszaros[2,7,8,9], Daniel Brumaru[2,6], Atish Mukherji[1,2], Sarah C. Durand[1,2], Laura Heydmann[1,2], Eloi R. Verrier[1,2], Hussein El Saghire[1,2], Nourdine Hamdane[1,2], Ralf Bartenschlager[10,11], Shaunt Fereshetian[12], Evelyn Ramberger[13,14], Rileen Sinha[3,4,5], Mohsen Nabian[3,4,5], Celine Everaert[3,4,5], Marko Jovanovic[12,15], Philipp Mertins[12,13,14], Steven A. Carr[12], Kazuaki Chayama[16,17], Nassim Dali-Youcef[2,6,7,8,9], Romeo Ricci[2,7,8,9], Nabeel M. Bardeesy[18], Naoto Fujiwara[19], Olivier Gevaert[4,20], Mirjam B. Zeisel[1,2], Yujin Hoshida[19], **Nathalie Pochet**[3,4,5], **Thomas F. Baumert**[1,2,21]

Author names in bold designate share co-first and co-last authorship

Affiliations:

[1]Institut National de la Santé et de la Recherche Médicale, U1110, Institut de Recherche sur les Maladies Virales et Hépatiques, Université de Strasbourg (IVH) Strasbourg F-67000, France, [2]Université de Strasbourg F-67000, France, [3]Department of Neurology, Harvard Medical School, Boston, MA 02115, USA, [4]Cell Circuits Program, Broad Institute of MIT and Harvard, Cambridge, MA 02142, USA, [5]Ann Romney Center for Neurologic Diseases, Brigham and Women's Hospital, Boston, MA 02115, USA, [6]Laboratoire de Biochimie et de Biologie Moléculaire, Pôle de biologie,

Hôpitaux Universitaires de Strasbourg, Strasbourg F-67091, France, [7]Institut de Génétique et de Biologie Moléculaire et Cellulaire, Illkirch F-67404, France, [8]Centre National de la Recherche Scientifique, UMR7104, Illkirch F-67404, France, [9]Institut National de la Santé et de la Recherche Médicale, U964, Illkirch F-67404, France, [10]Department of Infectious Diseases, Molecular Virology, Heidelberg University, D-69120 Heidelberg, Germany, [11]Division *Virus-Associated Carcinogenesis*, German Cancer Research Center (DKFZ), D-69120 Heidelberg, Germany, [12]The Broad Institute of Massachusetts Institute of Technology and Harvard, Cambridge, MA 02142, USA, [13]Proteomics Platform, Max Delbrück Center for Molecular Medicine in the Helmholtz Society, 13125 Berlin, Germany, [14]Berlin Institute of Health, 13125 Berlin, Germany, [15]Department of Biological Sciences, Columbia University, NY, USA, [16]Department of Gastroenterology and Metabolism, Applied Life Sciences, Institute of Biomedical & Health Sciences, Hiroshima University, Hiroshima, Japan, [17]Liver Research Project Center, Hiroshima University, Hiroshima, Japan, [18]Massachusetts General Hospital, Boston, MA 02114, USA, [19]Liver Tumor Translational Research Program, Simmons Comprehensive Cancer Center, Division of Digestive and Liver Diseases, Department of Internal Medicine, University of Texas Southwestern Medical Center, Dallas, TX 75390 USA, [20]Stanford Center for Biomedical Informatics Research (BMIR), Department of Medicine & Biomedical Data Science, Stanford University, CA 94305, USA, [21]Pôle Hépato-digestif, Institut Hopitalo-Universitaire, Strasbourg F-67000, France.

SUPPLEMENTARY MATERIALS AND METHODS

Reagents, antibodies and qPCR primers. All chemicals, the ECL reagent, Hyperfilms and Fluoroshield with 4′,6-diamidino-2-phenylindole (DAPI) were purchased from Sigma-Aldrich. Hepatitis B virus (HBV) surface antigen (HBsAg)-specific monoclonal antibody (NCL-HBsAg-2, clone 1044/341) was obtained from Leica Biosystems, recombinant human Interleukin–6 (IL-6) from Gibco, anti-catalase rabbit mAb (D4P7B), anti-STAT3 (9132) and anti-pSTAT3 Y705 (D3A7) from Cell Signaling Technology, anti-PPARA (H2) from Santa Cruz, anti-NS5A mouse mAb

(1827) from Virostat, anti-beta actin (AC-15) from Sigma, anti-rabbit IgG pAb (AF647) and anti-mouse IgG pAb (AF488) were obtained from Fisher Scientific. Generally, 20 µg of proteins were loaded for western blotting. cDNA was generated using Maxima first strand cDNA synthesis kit, Thermoscientific. qPCR was performed using a CFX96 real-time PCR system (BioRad) and iTaq Universal SYBR Green Supermix (BioRad) as recommended. If not indicated differently, all qPCR primers were synthetized by Sigma. Hepatitis C virus (HCV) genomes were quantified using SensiFAST Probe No-ROX One-Step Kit (Bioline) using JFH1 probes from Sigma (A221 and S147). Primer sequences to quantify albumin (ALB), hepatocyte nuclear factor 4 alpha (HNF4A), alpha-1-antitrypsin (A1AT) have been described[1]; CRAT (5'-GTA CCA CAG TGA CGG GAC AC-3', 5'-CCG GTT CAC CTT GTC TTT GAT-3'), EPHX2 (5'-GAC ATC GGG GCT AAT CTG AAG-3', 5'-GGC TTT ACT GTC ACG TAC CCA-3'), GAPDH (5'-TGC ACC ACC AAC TGC TTA-3', 5'-GGA TGC AGG GAT GAT GTT C-3') IDH1 (5'-TGT GGT AGA GAT GCA AGG AGA-3', 5'-TTG GTG ACT TGG TCG TTG GTG-3'), IL6-R (5'-CCC CTC AGC AAT GTT GTT TGT-3', 5'-CTC CGG GAC TGC TAA CTG G-3'). Catalase qPCR primer assay was obtained from Qiagen.

Virus strains, purification and titration. Cell culture-derived HCV (HCVcc) strains Jc1[2] and Jc1E2$^{FLAG\ 3}$ have been described. To generate a high-titer virus stock for proteomics experiments, culture medium containing FLAG-tagged HCVcc particles were collected daily starting two days after electroporation. 500 mL of cell culture supernatant were concentrated by ultracentrifugation (Vivaspin 20, MWCO 100,000, GE healthcare), purified using anti-FLAG M2 affinity gel (Sigma-Aldrich), and eluted with FLAG-peptide (Sigma-Aldrich). HCVcc infectivity was determined by calculating the 50 % tissue culture infective dose ($TCID_{50}$) as described[4]. Multiplicity of infection (MOI) was derived from the $TCID^{50}$ as described by the American Type Culture Collection (ATCC). HBV was produced by the cell line HepAD38 secreting infectious HBV (genotype D) into the culture medium. HBV enrichment and infection are described[5].

Inference of transcriptional regulatory networks

To infer the regulatory networks underlying the HCV-infected and non-infected Huh7.5.1^{dif} time courses, we analyzed the 21950 annotated genes from the RNA-Seq time course data (GEO dataset GSE126831) using the AMARETTO algorithm[6-8]. First, AMARETTO starts with selecting the top 50 % most varying genes across the samples in an unsupervised manner, which resulted in 10975 genes out of the 21950 annotated reference genes to be included in the analysis. From a predefined list of 4906 candidate regulators (Supplementary table S7/Input_regulators), 2720 candidate regulators were included in the analysis after the 50 % variation filtering. The AMARETTO algorithm subsequently identified 722 regulators (Supplementary table S7/Regulator_list_AMARETTO) of these candidate regulators as those putatively controlling the target genes in 150 modules of co-expressed target genes genome-wide using regularized regression. These modules were assessed for their enrichments in known functional categories from the MSigDB Hallmark and C2CP Collections[9]. The top scoring regulatory module 111 for enrichments in the HALLMARK_PEROXISOME signature genes is shown in Supplementary Fig. S7. AMARETTO's source code in R is available from GitHub (https://github.com/gevaertlab/AMARETTO and https://github.com/broadinstitute/CommunityAMARETTO) and user-friendly analysis modules are available from GenePattern (https://cloud.genepattern.org/ analysis modules 00378 and 00380).

SUPPLEMENTARY RESULTS

HCV induces an hepatic inflammatory response in quiescent Huh7.5.1 cells

Chronic inflammation of infected tissue is an important hallmark of HCV-induced pathogenesis contributing to fibrosis, cirrhosis and hepatocellular carcinoma (HCC). The innate antiviral response is triggered by double-stranded RNA (dsRNA) sensors RIG-I and MDA5 recognizing the viral genome and activating an antiviral program mediated by interferons and expression of

interferon-stimulated genes (ISGs). Only the cell lines Huh7.5.1 and its progenitor Huh7.5 can be efficiently infected by HCV in cell culture. This is due, at least in part, to an impaired capacity to activate interferon response[10, 11]. Despite these obeservations, in HCV-infected Huh7.5.1^{dif} we observe a robust induction of gene sets involved in interferon alpha response and inflammation (Supplementary Fig. S3) at the RNA level. Leading-edge genes involve the ISG *Mx1*, the expression of which is associated to HCV infection *in vivo*. Also, gene expression patterns of cytokines are strongly enriched in HCV-infected cells including the ISGs *IFIT1*, *IFIT3*, and *IFIT5* as leading-edge genes witnessing at least partially functional virus sensing and induction of an antiviral response (Supplementary table S2/All GSEA_anno (Huh7.5.1dif)). Consistently, we observe a significant enrichment of toll-like receptor (TLR) signaling and RIG-I/MDA5 pathways that are involved in dsRNA sensing. Leading-edge genes driving the enrichment include upregulated RIG-I (*DDX58*), MDA5 (*IFIH1*), and *TLR3* suggesting a partial rescue of the impaired RIG-I function by alternative sensors. A functional sensing of HCV in hepatocyte-like cells is also reflected by a strong *IRF3* gene expression on the RNA level (Supplementary table S1), which however did not translate into protein. This is consistent with general strong and significant enrichment of the interferon response pathways observed at the RNA level that is not found for the corresponding proteins and a strongly impaired expression of the RNA translation machinery in HCV-infected cells (Supplementary Fig. S3). Interestingly, while genes associated to translation are strongly impaired in the livers of HCV-infected patients and in Huh7.5.1^{dif} the same gene set it is positively enriched in the livers of the HCV-infected chimeric mice (Fig. S3, Supplementary table S3). This correlates with a more pronounced enrichment of interferon-response genes on the protein level in these chimeric livers. This further supports the conclusion that HCV infection overcomes the antiviral defense in hepatocytes mainly by inhibiting the translation of ISG mRNAs.

HCV-infected hepatocytes display a proteogenomic pattern resembling hallmarks for cancer development

Chronic HCV infection is a major risk factor of HCC suggesting virus-induced alterations of cancer-relevant pathways. Host signaling is not only required for HCV infection[12-14] but also persistent signals are transmitted by HCV infection that are involved in carcinogenesis[15]. Simultaneously, chronic HCV infection impairs cellular defense mechanisms of tumor development[16]. These data suggest a persistent mitogen-activated protein kinase (MAPK) and IL6/STAT3 signaling exerting a proliferative pressure onto the infected cell. Indeed, our proteogenomic atlas described here confirms this hypothesis and reveals a profound temporal activation of MAPK and STAT3 transcriptional signature in infected hepatocytes (Supplementary Fig. S6). At the same time, we observe an induction of hypoxia in infected cells (Fig. S6) that likely contributes to an amplification of HCV-induced epidermal growth factor receptor (EGFR) activation[15]. Moreover, overactivation of both pathways are hallmarks of carcinogenesis and functionally linked in human cancers[17]. As expected, we also observe a significant induction of epithelial to mesenchymal transition (EMT) in infected cells as previously linked to EGFR signaling in cancer[18] and HCV infection[19]. We found significantly decreased expression of components of the DNA repair machinery in infected cells (Supplementary Fig. S6) suggesting an increased genetic instability. Taken together, our proteogenomic data outline the oncogenic pressure in infected hepatocytes. Like an emergency break, the infected cell seems to arrest the cell cycle to counteract virus-induced proliferative signals and increased oxidative stress. However, repair mechanisms maintaining the genetic stability of the infected cell are impaired at the same time creating an imbalance that might promote carcinogenesis.

SUPPLEMENTARY FIGURES

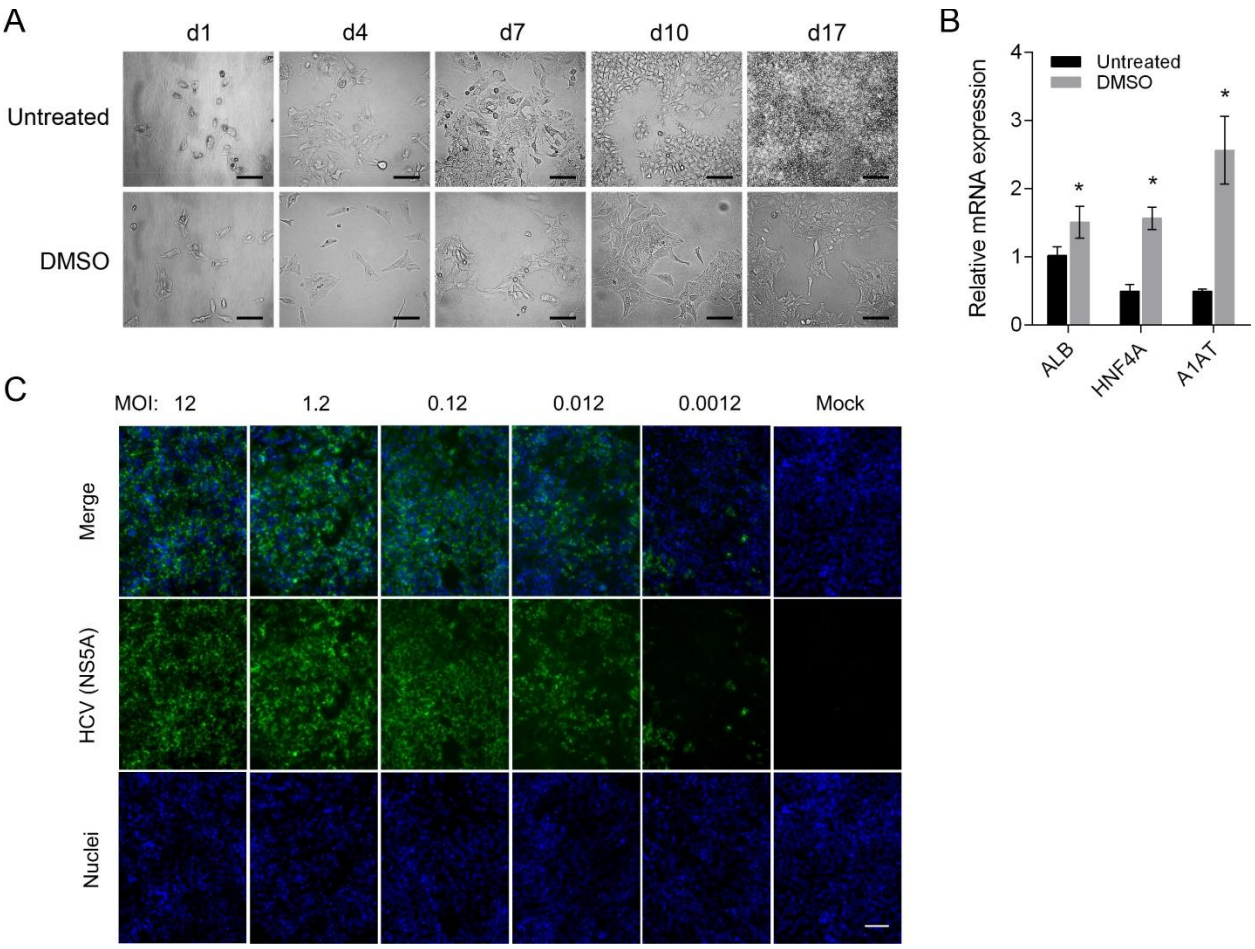

Fig. S1. Characterization and infection of DMSO-differentiated hepatocyte-like cells. (**A**) Cell culture with 1 % DMSO induces a re-differentiation of Huh7.5.1 cells into quiescent hepatocyte-like cells (Huh7.5.1^{dif}). (**B**) Huh7.5.1^{dif} display higher levels of hepatocyte-specific differentiation marker expression compared to untreated Huh7.5.1 cells. Bars represent relative mRNA expression compared to GAPDH measured by qPCR after 17 days treatment with 1 % DMSO (mean ± SD, three independent experiments in duplicates). Albumin (ALB), hepatocyte nuclear factor 4 alpha (HNF4A), alpha-1-antitrypsin (A1AT). (**C**) Huh7.5.1 cells were incubated with 1 % DMSO for 10 days prior infection with HCVcc (strain Jc1E2^{FLAG}) for additional 7 days in the presence of 1 % DMSO. Cells were infected at a MOI of 12 or dilutions of the same virus preparation. Nuclei were visualized by DAPI staining of cellular DNA; HCV infection by NS5A staining. Bar represents 200 µm.

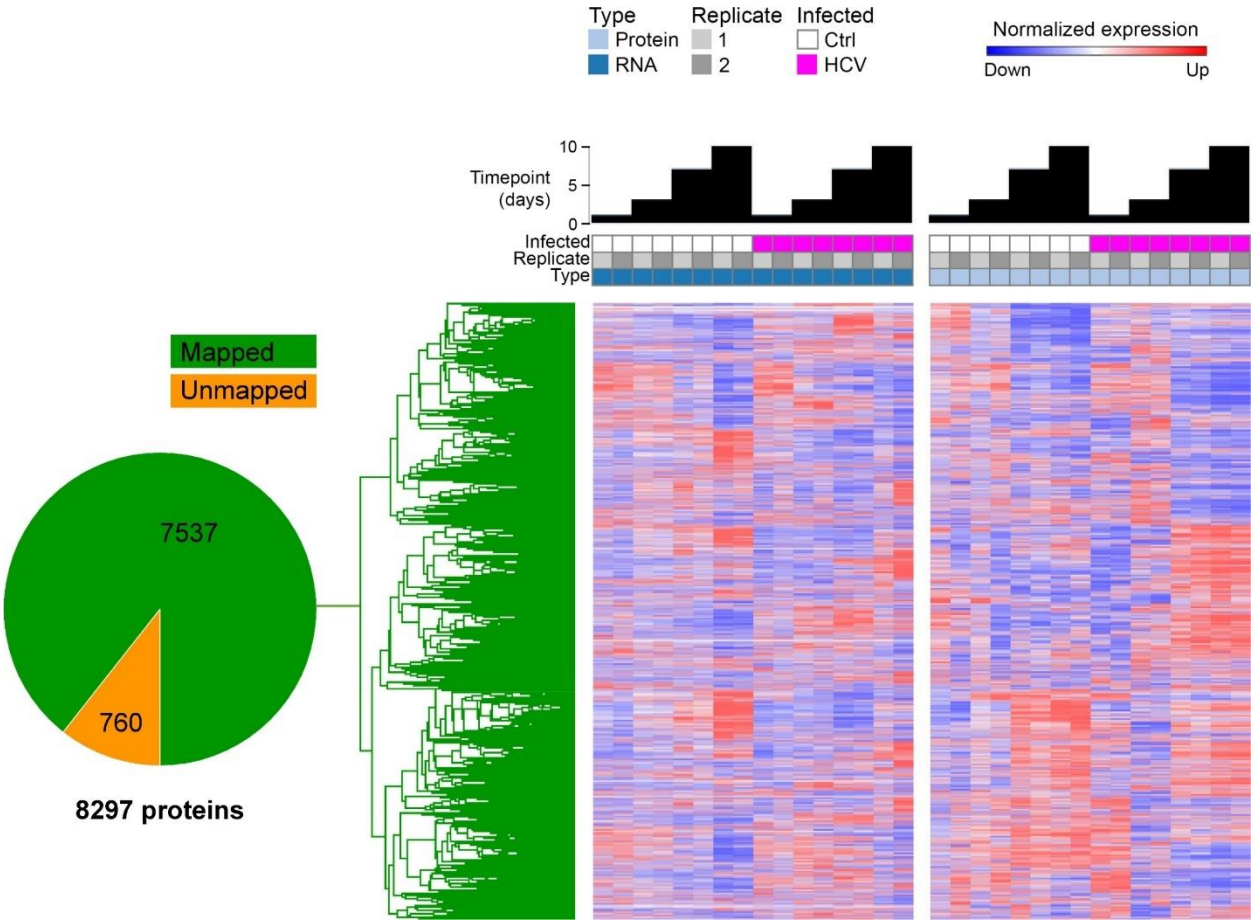

Fig. S2. Highly reproducible mapping of proteomics to mRNA transcripts in HCV-infected liver cells. 8,297 proteins were altered during HCV infection. 7,537 (green) were mapped to corresponding mRNAs of the same experiment. The heatmap clustering of the mapped and normalized mRNA and protein expression emphasizes the high reproducibility of the two biological replicates.

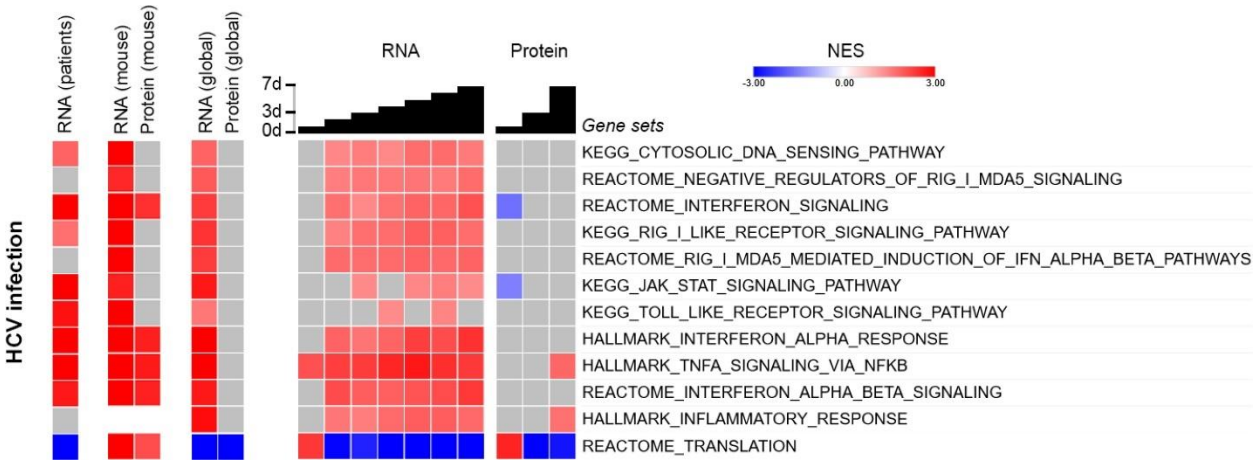

Fig. S3. Persistent HCV infection triggers an attenuated innate immune response. HCV-infected Huh7.5.1^{dif} cells relative to mock-infected cells until 7 days pi. GSEA of proteomics and/or transcriptomics of livers of HCV-infected patients, human liver chimeric uPA/SCID mice, and Huh7.5.1^{dif}. HCV infection induces RNA expression of genes associated to innate immunity but suppresses their translation into proteins. NES are displayed in red (increased), blue (decreased), gray (no significant change), and white (below analysis cut-off). Temporal analysis of infected Huh7.5.1^{dif} are presented as global trend (global) and individual timepoints. Statistical cut-off for GSEA of liver tissues was FDR q<0.05 and for infected Huh7.5.1^{dif} p<0.005).

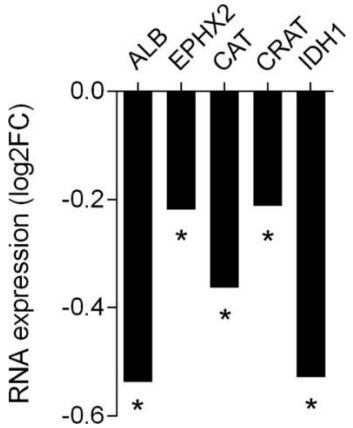

Fig. S4. Expression of leading-edge genes of the HALLMARK_PEROXISOME gene set are impaired by HCV infection. Validation of top five genes (Huh7.5.1^{dif}, RNA-seq) shown in Figure 3B using quantitative PCR. Data displayed as log2FC RNA expression in HCV infected Huh7.5.1^{dif} cells. GAPDH expression was used as housekeeping gene. * p<0.05, one-tailed T-Test (n=3 in duplicates).

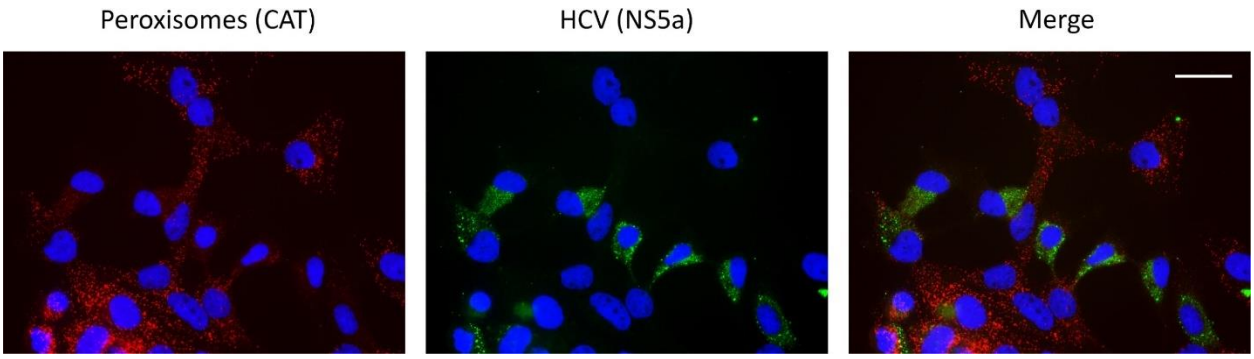

Fig. S5. Peroxisome maker expression is perturbed in HCV-infected hepatocyte-like cells. Immunofluorescence microscopy of Huh7.5.1^{dif} cells infected for 3 days with HCVcc. The peroxisomal marker catalase (CAT) is stained in red, nuclear DNA (DAPI) in blue and HCV (NS5A) in green. Bar represents 200 µm.

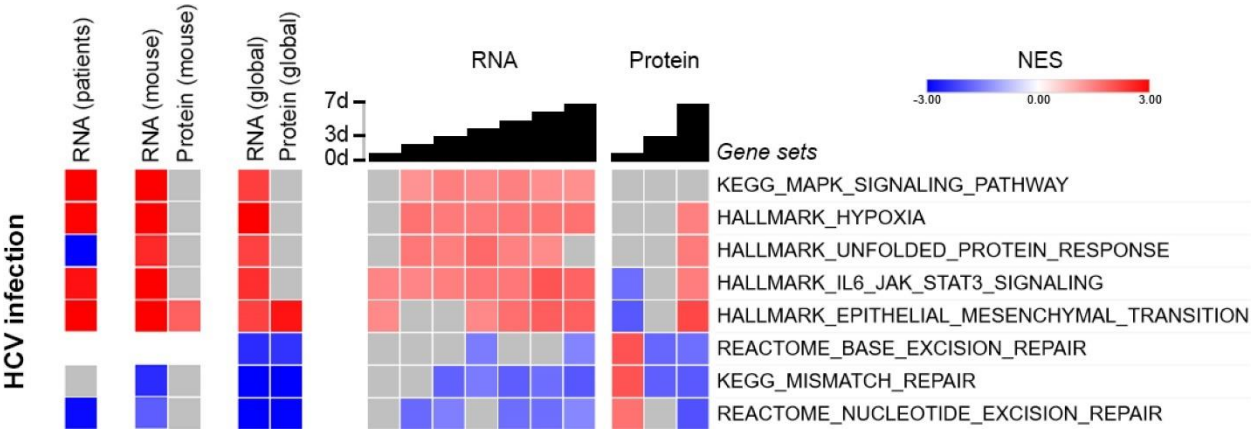

Fig. S6. Persistent HCV infection perturbs cell circuits driving liver disease and cancer. GSEA of transcriptomics and proteomics of HCV-infected Huh7.5.1^{dif} cells relative to mock-infected cells until 7 days pi. HCV infection perturbs pathways that are known hallmarks of cancer development. NES are displayed in red (increased), blue (decreased), gray (no significant change), and white (below analysis cut-off). Temporal analysis of infected Huh7.5.1^{dif} are presented as global trend (global) and individual timepoints. Statistical cut-off for GSEA of liver tissues was FDR q<0.05 and for infected Huh7.5.1^{dif} p<0.005).

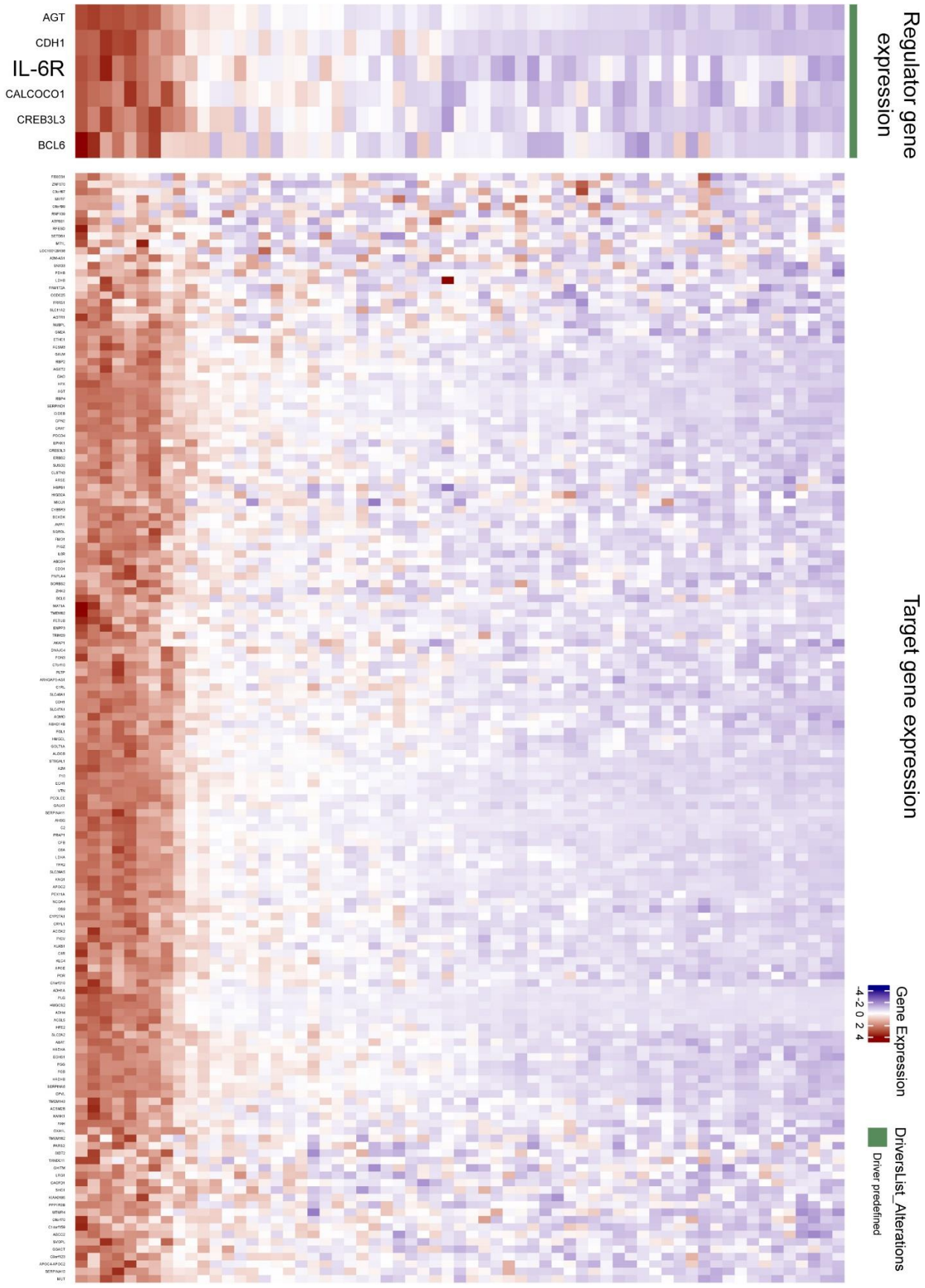
AGT
CDH1
IL-6R
CALCOCO1
CREB3L3
BCL6
Regulator gene expression
Target gene expression
Gene Expression
-4 -2 0 2 4
DriversList_Alterations
Driver predefined

Fig. S7. IL-6 receptor is a predicted regulator of peroxisomal function. The top-scoring regulatory module (#111) inferred by the AMARETTO algorithm for enrichments in peroxisomal function (HALLMARK_PEROXISOME signature genes). The heatmap of the regulatory module shows the regulators that act together in a regulatory program (top heatmap) and the co-expressed target genes (bottom heatmap) that they putatively control. IL-6R is one of 6 regulators that together best predict the target genes' expression in this regulatory module. Enrichments in known functional categories from the MSigDB Hallmark and C2CP Collections are summarized in Supplementary table S6.

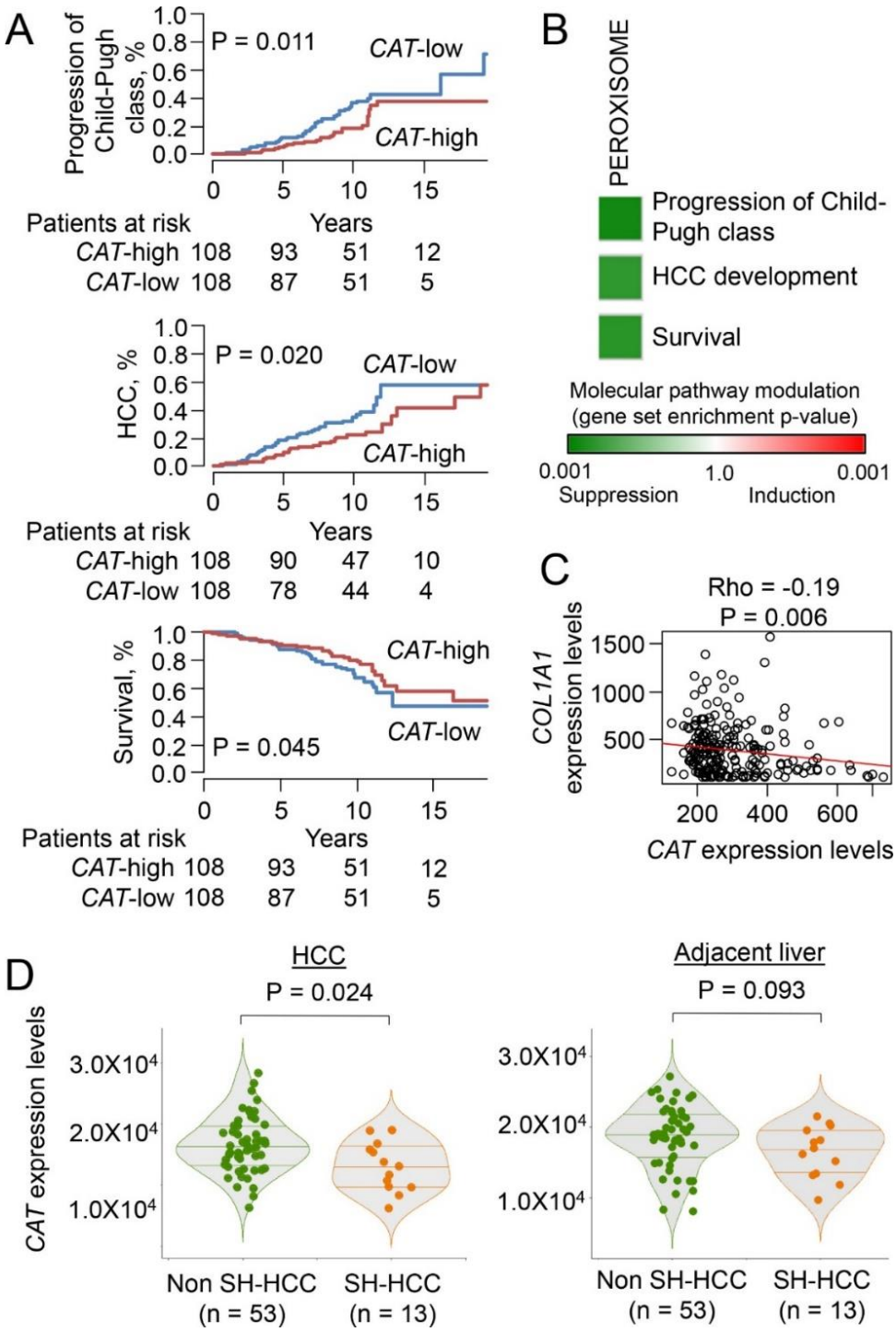

Fig. S8. Significant association of hepatic catalase expression with clinical outcomes and phenotypes in viral and metabolic liver disease. (**A**) Early-stage HCV cirrhosis patients (n=216)[20] are classified into 2 groups, i.e., *CAT*-high and low groups, based on median expression level. Association of the grouping with overall survival (bottom), HCC development (middle), and progression of Child-Pugh class[21] from A to B or C (top). Patients with lower *CAT* expression

show worse clinical outcomes (log-rank test). (**B**) Association of peroxisome pathway modulation with the clinical outcomes in the 216 HCV cirrhosis patients determined by GSEA. (**C**) *CAT* expression levels were negatively correlated (Spearman correlation test) with hepatic *COL1A1* expression levels in the 216 HCV cirrhosis patients. (**D**) Distribution and probability density of *CAT* expression in HCC tumor (left) and adjacent non-tumor liver tissues (right) in 66 HCC patients[22] according to presence of histological steatohepatitic HCC (SH-HCC) variant[23] (violin plot, Wilcoxon rank-sum test). *CAT*= catalase, peroxisomal marker.

SUPPLEMENTARY TABLES

Supplementary Table S1. Mapped RNAs and proteins. HCV-infected Huh7.5.1^{dif}. Expression levels included are displayed in log2FC. Baseline protein expression levels of non-infected cells (sheet Protein mapped log2FC) are displayed as peptide precursor intensity based. *[online Supplementary table]*

Supplementary Table S2. GSEA of proteogenomics analysis, annotations and leading edge genes. Geneset enrichment results of the heatmaps displayed in this study including HCV-infected Huh7.5.1^{dif} and liver tissues of HCV-infected patients and chimeric mice. *[online Supplementary table]*

Supplementary Table S3. Proteome from livers of HCV-infected chimeric mice. Identified proteome of human part only (liver repopulation by human hepatocytes ~80-90 % according to human albumin level >10 mg/mL). Bold column represent log2 fold change (log2FC) of HCV-infected mice (n=5) vs. Mock-infected mice (n=5), baseline expression levels are displayed in peptide precursor intensity based. *[online Supplementary table]*

Supplementary Table S4. HCV-induced changes of polar metabolite abundance. Huh7.5.1^{dif} cells infected with HCVcc for 7 days. Intracellular polar metabolites quantified by mass spectroscopy. FC, fold change; SD, standard deviation. p value represent T-Test of triplicates.

Polar metabolite	FC	SD	p
Citrate	3.13	0.14	0.0006
Tyrosine	6.41	1.87	0.0038
Succinate	7.31	2.55	0.0068
Valine	7.94	3.47	0.0129
Leucine	9.43	4.55	0.0163
Serine	-3.56	0.24	0.0181
Glycine	4.41	1.88	0.0181
3-Phosphoglycerate	4.67	2.05	0.0198
Malate	-1.58	0.13	0.0206
Pyr	4.19	1.88	0.0211
Phenylalanine	3.35	1.32	0.0222
Methionine	3.35	1.32	0.0223
Isoleucine	9.62	5.33	0.0244
Aspartate	-1.59	0.05	0.0355
Lactate	3.13	1.57	0.0392
Glutamate	2.04	0.90	0.0611
Alanine	2.55	1.41	0.0655
Lysine	-1.50	0.17	0.0848
Threonine	3.12	2.32	0.0947
Glutamine	-1.32	0.52	0.2439
Proline	-1.12	0.49	0.3617
pSerine	1.10	1.09	0.4457
aKG	-1.01	0.23	0.4827

Supplementary Table S5. Predicted transcription factors involved in peroxisomal regulation. (Sheet *Enrichr*) Transcription factor binding sites potentially involved in peroxisomal regulation. Top 30 transcription factor binding sites (excluding duplicates) among the combined 85 leading edge genes of the HALLMARK_PEROXISOME gene set in livers of HCV-infected patients and Huh7.5.1^{dif} cells by using Enrichr. (Sheet *HCV-modulated regulators*) HCV-induced deregulation of potential transcription factors. Log2 fold change at day 7 p.i. Unmapped RNAseq dataset of HCV-regulated modulators. *[online Supplementary table]*

Supplementary Table S6. Functional enrichments of AMARETTO Module 111 in the MSigDB Hallmark and C2CP Collections. Functional categories are sorted by p-value, threshold: p<0.05 and min. 2 overlapping genes. *[online Supplementary table]*

Supplementary Table S7. List of known regulators used for AMARETTO analysis. (sheet *Input_regulators*) List of recognized genetic regulators that were used as input to AMARETTO prior selection. (sheet *Regulator_list_AMARETTO*) Regulator list used for the prediction after filtering variance and penalized regression by AMARETTO. *[online Supplementary table]*

Supplementary Table S8. Clinical demographics of early-stage HCV cirrhosis cohort. IQR, interquartile range; SVR, sustained virologic response; IQR, interquartile range; ALT, alanine aminotransferase. * The number (%) was calculated in a subset of 94 patients who had history of interferon-based anti-HCV therapies and antiviral response information.

	Overall (*n*=216)	Impaired peroxisomal function (*n*=23)	Intact peroxisomal function (*n*=193)	p
Age, median (IQR)	59 (54-64)	59 (54-64)	59 (54-64)	0.67
Sex, male, *n* (%)	116 (54)	12 (52)	104 (54)	1.00
Esophageal or gastric varices (F1/F2/F3), n	42/9/1	11/1/0	31/8/1	0.003
Progression of Child-Pugh class, n (%)	66 (31)	13 (57)	53 (27)	0.007
Alanine aminotransferase (*IU*), median (IQR)	108 (63-167)	125 (96-157)	106 (62-169)	0.40
Diabetes, *n* (%)	24 (11)	2 (9)	22 (11)	1.00
Hypertension, *n* (%)	10 (5)	0 (0)	10 (5)	0.60
Genotype 1b, n (%)	122 (58)	17 (74)	105 (56)	0.12
History of Interferon-based treatment, *n* (%)	101 (47)	12 (52)	89 (46)	0.66
Achievement of SVR, *n* (%)*	21 (22)	2 (18)	19 (23)	1.00

Supplementary Table S9. Clinical demographics of HCC cohort. SH-HCC, steatohepatitic hepatocellular carcinoma; AST, aspartate aminotransferase; IQR, interquartile range.

	Overall (*n*=66)	SH-HCC (*n*=12)	Non SH-HCC (*n*=54)	p
Age, median (IQR)	57 (52-63)	55 (50-58)	58 (52-64)	0.26
Sex, male, *n* (%)	50 (76)	10 (83)	40 (74)	0.72
Platelet count <100x10^3/mL, n (%)	22 (33)	4 (33)	18 (33)	1.00
AST (IU), median (IQR)	38 (24-57)	51 (29-155)	38 (25-57)	0.31
Albumin (g/dL), median (IQR)	3.8 (3.6-4.1)	4.1 (3.8-4.2)	3.8 (3.6-4.1)	0.074
Bilirubin (mg/dL), median (IQR)	1.0 (0.8-1.5)	1.2 (0.9-1.3)	1.0 (0.8-1.6)	0.99
Prothrombin time (%), median (IQR)	89 (81-100)	90 (82-97)	89 (81-101)	0.58
Child-Pugh class (A/B), n	58/8 (88/12)	11/1 (92/8)	47/7 (87/13)	1.00

REFERENCES IN SUPPLEMENTARY INFORMATION

1. Sainz B, Jr., Chisari FV. Production of infectious hepatitis C virus by well-differentiated, growth-arrested human hepatoma-derived cells. J Virol 2006;80:10253-7.
2. Pietschmann T, Kaul A, Koutsoudakis G, et al. Construction and characterization of infectious intragenotypic and intergenotypic hepatitis C virus chimeras. Proc Natl Acad Sci U S A 2006;103:7408-13.
3. Merz A, Long G, Hiet MS, et al. Biochemical and morphological properties of hepatitis C virus particles and determination of their lipidome. J Biol Chem 2011;286:3018-32.
4. Zeisel MB, Koutsoudakis G, Schnober EK, et al. Scavenger receptor class B type I is a key host factor for hepatitis C virus infection required for an entry step closely linked to CD81. Hepatology 2007;46:1722-31.
5. Verrier ER, Yim SA, Heydmann L, et al. Hepatitis B Virus Evasion From Cyclic Guanosine Monophosphate-Adenosine Monophosphate Synthase Sensing in Human Hepatocytes. Hepatology 2018;68:1695-1709.
6. Champion M, Brennan K, Croonenborghs T, et al. Module Analysis Captures Pancancer Genetically and Epigenetically Deregulated Cancer Driver Genes for Smoking and Antiviral Response. EBioMedicine 2018;27:156-166.
7. Gevaert O. MethylMix: an R package for identifying DNA methylation-driven genes. Bioinformatics 2015;31:1839-1841.
8. Gevaert O, Villalobos V, Sikic BI, et al. Identification of ovarian cancer driver genes by using module network integration of multi-omics data. Interface Focus 2013;3:20130013.
9. Subramanian A, Tamayo P, Mootha VK, et al. Gene set enrichment analysis: a knowledge-based approach for interpreting genome-wide expression profiles. Proc Natl Acad Sci U S A 2005;102:15545-50.

10. Binder M, Kochs G, Bartenschlager R, et al. Hepatitis C virus escape from the interferon regulatory factor 3 pathway by a passive and active evasion strategy. Hepatology 2007;46:1365-74.
11. Sumpter R, Jr., Loo YM, Foy E, et al. Regulating intracellular antiviral defense and permissiveness to hepatitis C virus RNA replication through a cellular RNA helicase, RIG-I. J Virol 2005;79:2689-99.
12. Lupberger J, Van Renne N, Baumert TF. Signaling of hepatitis C virus. In: Dufour JF, Clavien PA, eds. Signaling Pathways in Liver Disease. 3rd ed: Wiley Blackwell, 2015:459-68.
13. Lupberger J, Zeisel MB, Xiao F, et al. EGFR and EphA2 are host factors for hepatitis C virus entry and possible targets for antiviral therapy. Nat Med 2011;17:589-95.
14. Zona L, Lupberger J, Sidahmed-Adrar N, et al. HRas signal transduction promotes hepatitis C virus cell entry by triggering assembly of the host tetraspanin receptor complex. Cell Host Microbe 2013;13:302-13.
15. Mailly L, Xiao F, Lupberger J, et al. Clearance of persistent hepatitis C virus infection in humanized mice using a claudin-1-targeting monoclonal antibody. Nat Biotechnol 2015;33:549-554.
16. Van Renne N, Roca Suarez AA, Duong FHT, et al. miR-135a-5p-mediated downregulation of protein tyrosine phosphatase receptor delta is a candidate driver of HCV-associated hepatocarcinogenesis. Gut 2018;67:953-962.
17. Franovic A, Gunaratnam L, Smith K, et al. Translational up-regulation of the EGFR by tumor hypoxia provides a nonmutational explanation for its overexpression in human cancer. Proc Natl Acad Sci U S A 2007;104:13092-7.
18. Misra A, Pandey C, Sze SK, et al. Hypoxia activated EGFR signaling induces epithelial to mesenchymal transition (EMT). PLoS One 2012;7:e49766.

19. Li Q, Sodroski C, Lowey B, et al. Hepatitis C virus depends on E-cadherin as an entry factor and regulates its expression in epithelial-to-mesenchymal transition. Proc Natl Acad Sci U S A 2016;113:7620-5.

20. Hoshida Y, Villanueva A, Sangiovanni A, et al. Prognostic gene expression signature for patients with hepatitis C-related early-stage cirrhosis. Gastroenterology 2013;144:1024-30.

21. Pugh RN, Murray-Lyon IM, Dawson JL, et al. Transection of the oesophagus for bleeding oesophageal varices. Br J Surg 1973;60:646-9.

22. Hoshida Y, Villanueva A, Kobayashi M, et al. Gene expression in fixed tissues and outcome in hepatocellular carcinoma. N Engl J Med 2008;359:1995-2004.

23. Tan PS, Nakagawa S, Goossens N, et al. Clinicopathological indices to predict hepatocellular carcinoma molecular classification. Liver Int 2016;36:108-18.